OPEN

Citation: Cell Death and Disease (2013) 4, e751; doi:10.1038/cddis.2013.274

www.nature.com/cddis

PKC-dependent ERK phosphorylation is essential for $P2X_7$ receptor-mediated neuronal differentiation of neural progenitor cells

H-K Tsao[1], P-H Chiu[1] and SH Sun*,[1]

Purinergic receptors have been shown to be involved in neuronal development, but the functions of specific subtypes of P2 receptors during neuronal development remain elusive. In this study we investigate the distribution of $P2X_7$ receptors ($P2X_7$Rs) in the embryonic rat brain using *in situ* hybridization. At E15.5, $P2X_7$R mRNA was observed in the ventricular zone and subventricular zone, and colocalized with nestin, indicating that $P2X_7$R might be expressed in neural progenitor cells (NPCs). $P2X_7$R mRNA was also detected in the subgranular zone and dentate gyrus of the E18.5 and P4 brain. To investigate the roles of $P2X_7$R and elucidate its mechanism, we established NPC cultures from the E15.5 rat brain. Stimulation of $P2X_7$Rs induced Ca^{2+} influx, inhibited proliferation, altered cell cycle progression and enhanced the expression of neuronal markers, such as TUJ1 and MAP2. Similarly, knockdown of $P2X_7$R by shRNA nearly abolished the agonist-stimulated increases in intracellular Ca^{2+} concentration and the expression of TUJ1 and NeuN. Furthermore, stimulation of $P2X_7$R induced activation of ERK1/2, which was inhibited by the removal of extracellular Ca^{2+} and treatment with blockers for $P2X_7$R and PKC activity. Stimulation of $P2X_7$R also induced translocation of PKCα and PKCγ, but not of PKCβ, whereas knockdown of either PKCα or PKCγ inhibited ERK1/2 activation. Inhibition of PKC or p-ERK1/2 also caused a decrease in the number of TUJ1-positive cells and a concomitant increase in the number of GFAP-positive cells. Taken together, the activation of $P2X_7$R in NPCs induced neuronal differentiation through a PKC-ERK1/2 signaling pathway.
Cell Death and Disease (2013) **4,** e751; doi:10.1038/cddis.2013.274; published online 1 August 2013
Subject Category: Neuroscience

The determination of neuronal and glial fate during CNS development involves complex interactions of intrinsic signals through many transcription factors.[1] Neural stem cells (NSCs) have been considered as primary progenitor cells that lead to the formation of neuronal or glial cell lineages during development.[2] NSCs are multipotent stem cells that exist in prenatal and early postnatal stages in two zones, the ventricular zone (VZ) and the subventricular zone (SVZ).[3] NSCs develop into immediate progeny that are known as neural progenitor cells (NPCs),[4] which have limited self-renewal capacity, behave as transient amplifying cells and have a higher rate of differentiation compared with NSCs.[5]

Growth and proliferation of NPCs require short-range autocrine/paracrine signals and the NPCs to be in close contact with one another. It has been suggested that one such short-range pathway is the ATP signaling. Purinergic receptors have been classified into two major families: P2Y and P2X receptors. Purinergic receptors have been shown to express in the early embryonic brain and have a role in embryogenesis.[6] ATP acts as a proliferation signal for NPCs and also as a negative regulator of terminal neuronal differentiation through P2Y receptors.[7] In addition, ATP has been shown to promote cell–cell communication and embryogenesis via stimulation of increases in intracellular Ca^{2+} concentration ($[Ca^{2+}]_i$).[8,9] ATP has also been found to enhance proliferation by elevating $[Ca^{2+}]_i$ in olfactory epithelium.[10] Thus, ATP-mediated Ca^{2+} signaling may have a crucial role in neurogenesis through regulation of differentiation, migration and cell fate determination.

Unlike other P2X receptor subtypes, the $P2X_7$ receptor ($P2X_7$R) has a short intracellular N-terminal domain, two transmembrane domains and a long C-terminal domain.[11] Activation of $P2X_7$Rs is known to induce Ca^{2+} influx and gliotransmitter release in astrocytes.[12,13] Expression of $P2X_7$Rs has been identified in neurons and activation of the receptor results in glutamate-mediated excitation.[14] $P2X_7$Rs can be found in growth cones and can modulate neurotransmitter release in neurons.[15] Recent studies have shown that the inhibition of $P2X_7$R improves recovery after spinal cord injury and promotes axonal growth in hippocampal neurons.[16,17] Thus, $P2X_7$Rs may have an important role in neuronal growth and regeneration.

Although the transcriptional and epigenetic factors involved in determination of NPCs fate have been well characterized, $P2X_7$R-mediated extracellular cues in NPCs remain unexamined. A previous report indicated that the expression of $P2X_7$Rs was found from E14 onward in rat embryos and triggered Ca^{2+} wave in the VZ of E16 brain.[6,18] Adult NPCs have also been found to express $P2X_7$Rs, and their stimulation evoked an inward current and membrane depolarization.[19] In this study we investigate the expression of $P2X_7$Rs in E15,

[1]Institute of Neuroscience and Brain Research Center, National Yang-Ming University, Taiwan, Republic of China
*Corresponding author: SH Sun Institute of Neuroscience, National Yang Ming University, No. 155, Section 2, Linong Street, Taiwan, Republic of China. Tel: +886 2 2826 7103; Fax: +886 2 2820 0259; E-mail: shsun@ym.edu.tw
Keywords: $P2X_7$R; MAPKs; neural differentiation; Ca^{2+} flux; PKC
Abbreviations: NPC, neural progenitor cell; SVZ, subventricular zone; $P2X_7$R, $P2X_7$ receptor; oATP, oxidized ATP
Received 18.4.13; revised 19.6.13; accepted 21.6.13; Edited by A Verkhratsky

E18 and P4 rat brain, and examine the mechanism involved in the P2X$_7$R-mediated neuronal differentiation of NPCs established from the E15.5 rat brain. We demonstrated that P2X$_7$R is expressed in VZ and SVZ of the E15, E18 and P4 rat brain, and that stimulation of the receptors on the NPCs induces neuronal differentiation via the PKC-ERK1/2 signaling pathway.

Results

P2X$_7$R RNA is expressed in the developing rat brain. In the present study we examined the expression of P2X$_7$R mRNA using *in situ* hybridization (ISH) and the expression of neuronal markers using immunohistochemistry (IHC). Our preliminary results revealed that P2X$_7$R mRNA was predominantly expressed in the cerebral cortex, basal ganglia and thalamus in the E15.5 rat brain (Supplementary Figure 1A); therefore, we focused our analysis on these areas. As shown in Figure 1a, enrichment of P2X$_7$R mRNA was observed in the VZ and SVZ of the E15.5 rat brain and colocalized with nestin expression in these areas. P2X$_7$R mRNA expression was also found to colocalize with TUJ1 expression in the SVZ of the E15.5 brain (Figure 1b). However, in the E18.5 (Figure 1c) and P4 (Figure 1d) rat

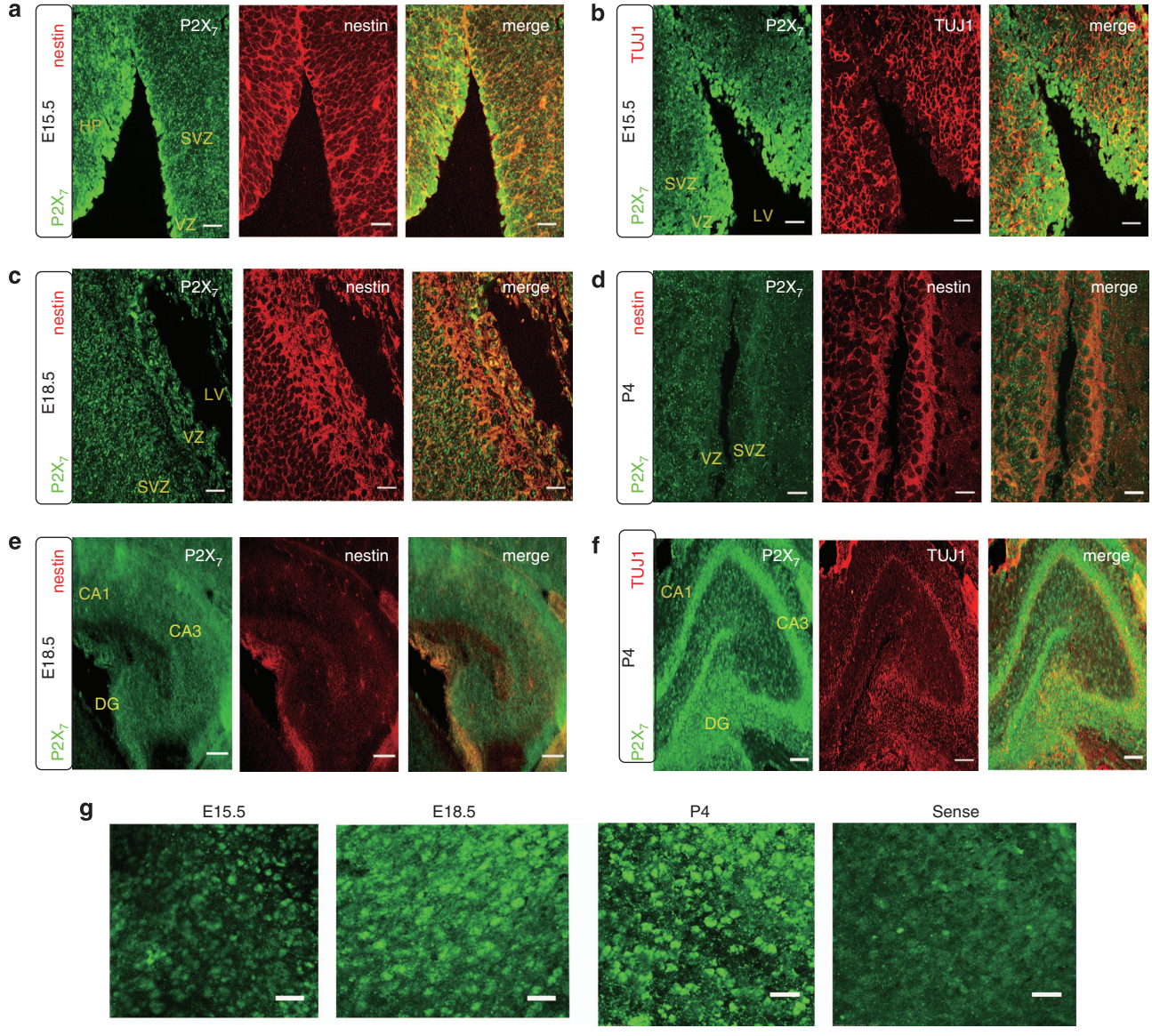

Figure 1 Embryonic rat brain expresses P2X$_7$R. Photomicrographs of the coronal sections of the SVZ and hippocampus were taken at different developmental stages, and were stained with ISH for P2X$_7$R mRNA and with IHC for the cell markers nestin and TUJ1. E15.5 embryonic brains were stained for P2X$_7$R (green) and nestin (red) (**a**), and for P2X$_7$R (green) and TUJ1 (red) (**b**); SVZ, subventricular zone; VZ, ventricular zone; LV, lateral ventricle. The SVZ and VZ in the E18 (**c**) and P4 (**d**) rat brain were stained for P2X$_7$R (green) and nestin (red). Scale bar: 100 μM. The CA1-CA3 and DG of the hippocampus at E18.5 (**e**) and P4 (**f**) rat brain were stained for P2X$_7$R (green) and nestin (red). Scale bar: 200 μM; DG, dentate gyrus. (**g**) Higher-magnification photomicrographs of ISH for antisense P2X$_7$R probe were stained in the cortical plate of the E15.5, E18.5 and P4 brains, and for the sense P2X$_7$R probe at P4 brains. Scale bar: 20 μM

brains, few nestin-positive cells were observed to colocalize with P2X$_7$R mRNA in the VZ. Furthermore, P2X$_7$R mRNA colocalized with nestin in the E18.5 hippocampus (Figure 1e) and colocalized with TUJ1 in CA1 and CA3, as well as in the granule cell layer and subgranular zone (SGZ) of dentate gyrus (DG) in the hippocampus at P4 (Figure 1f). Higher-magnification microscopic analysis revealed that P2X$_7$R mRNA expression was more abundant in the cortical cells of the P4 brain than that of E15.5 brain (Figure 1g). These results showed that P2X$_7$R mRNA is generally expressed in nestin-positive NPCs in the developing rat brain. Our results further showed that P2X$_7$R mRNA is also expressed in terminally differentiated neural cells at E18.5.

P2X$_7$R negatively regulates NPC proliferation. To further investigate the roles of P2X$_7$Rs in VZ and SVZ, we established NPC cultures using cells isolated from the E15.5 rat brain. RT-PCR analysis revealed that these cells expressed P2X$_7$R mRNA (Figure 2a). Ca^{2+} imaging analysis revealed that a potent P2X$_7$R agonist, BzATP, stimulated increase in $[Ca^{2+}]_i$ (Figure 2b) that was abolished by the removal of Ca^{2+} in the medium and was inhibited by the selective P2X$_7$R antagonists, A438079, oxidized ATP (oATP), Brilliant Blue G (BBG) and calmidazolium (Figure 2c). Thus, BzATP might stimulate Ca^{2+} influx through P2X$_7$R. RT-PCR analysis indicated NPCs also express other P2 receptors and a higher concentration of ATP-stimulated increases in $[Ca^{2+}]_i$ (Supplementary Figures 2A and B). To ascertain that the BzATP did not activate other P2 receptors of NPCs, we measure Ca^{2+} response in the presence of P2X, P2X$_4$R, P2Y$_1$R, P2YR, and P2X$_{1-6}$R antagonists, PPADS, 5BDBD, MRS2179, suramin and TNP-ATP respectively. The results revealed that only PPADS inhibited BzATP-stimulated Ca^{2+} signal (Supplementary

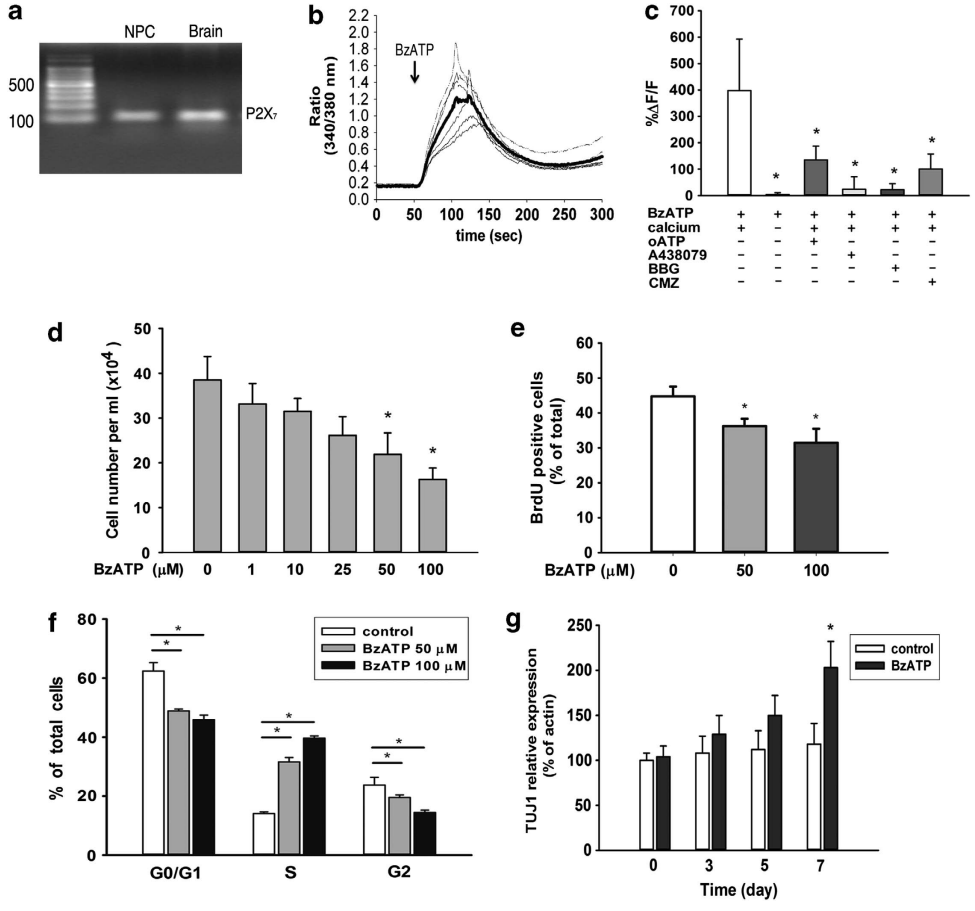

Figure 2 Stimulation of P2X$_7$R inhibits proliferation and alters cell cycle progression but does not cause cell death in NPCs. (**a**) RT-PCR analysis of P2X$_7$R mRNA expression in NPCs and E15 rat brain. (**b**) The NPCs were loaded with fura-2 AM and stimulated with BzATP. The bold line represents an averaged trace of the Ca^{2+} signal ($n=11$). (**c**) $[Ca^{2+}]_i$ was calculated by subtracting the peak level from the basal level with ($+$) or without ($-$) extracellular Ca^{2+} or the P2X$_7$ antagonists, 20 μM A438079, 10 μM oATP, 1 μM BBG or 5 μM calmidazolium (CMZ, $n=5$). *Significantly different means ($P<0.05$) using Mann–Whitney's *U*-test for comparison with BzATP. (**d**) BzATP dose-dependently affects the number of NPCs. The dissociated cells were treated with 1–100 μM BzATP for 4 days and were counted by a hemocytometer ($n=3$). *$P<0.05$ using Bonferroni's post test for comparison with the respective controls. (**e**) Photomicrographs of NPCs incubated in the presence or absence of BzATP for 4 days, labeled with BrdU for 8 h, counter-stained with DAPI and imaged. The results represent BrdU-positive cell percentages of total cells. (**f**) NPCs were treated with BzATP for 4 days and then labeled with PI, and the number of cells in each stage of the cell cycle was analyzed by flow cytometry. Comparison of results and statistical analysis ($n=3$). *$P<0.05$ using nonpaired Student's *t*-test for comparison with the respective controls. (**g**) NPCs were analyzed by western blot analysis for TUJ1 expression after treatment with BzATP (0, 3, 5 and 7 days). Quantitative analyses represent percentages of TUJ1-expression to actin. Actin (1:2000) was purchased from Life Technologies. *$P<0.05$ using Bonferroni's post test for comparison with the respective controls

Figure 2C). This demonstrated that BzATP only activates P2X$_7$R in NPCs. In addition, treatment of the NPC cultures with BzATP (1–100 μM) for 4 days decreased the cell number dose dependently (Figure 2d). The BzATP treatment also decreased 5-bromo-2′-deoxyuridine (BrdU) incorporation of the spheres, and the statistical analyses revealed this decrease was dose dependent (Figure 2e). We conducted TUNEL assays to investigate whether the decreases in BrdU incorporation might be due to cell death. BzATP did not induce cell death compared with the controls, suggesting that the reduction in cell number could not be attributed to apoptosis (Supplementary Figure 3A). Flow cytometry analysis further revealed that BzATP treatment had no effect on the sub-G1 phase (Supplementary Figure 4A) but altered cell cycle progression by decreasing cells in the G0/G1 and G2 phases, and increased the number of cells in the S phases of these cells (Figure 2f). Thus, activation of P2X$_7$R induced a negative regulation of proliferation and might increase the neuronal differentiation of NPCs.

Stimulation of P2X$_7$R enhances the neuronal differentiation of NPCs. To examine whether the activation of P2X$_7$R induces the neuronal differentiation of NPCs, we analyzed the BzATP-stimulated TUJ1 expression via western blot analysis. Our preliminary analysis revealed that BzATP treatment induced increases in the TUJ1 expression, and a statistically significant increase was observed at day 7 (Figure 2g). We therefore analyzed NPC and neuronal marker expression by treating NPCs with 50 μM BzATP for 7 days. We first stained the dispersed naive NPCs for GFAP and nestin expression. As shown in Figure 3a, the dispersed NPCs stained intensely for GFAP and nestin, but much more weakly for TUJ1 and MAP2. Treatment of BzATP enhanced the expression of TUJ1 and MAP2 (Figure 3b). The BzATP-enhanced expression of TUJ1 and MAP2 was inhibited by the P2X$_7$R antagonists, oATP (Figure 3c) and A438079 (Figure 3d). The statistical analysis showed that BzATP treatment decreased the numbers of nestin-positive cells and enhanced the TUJ1- and MAP2-positive cells, and

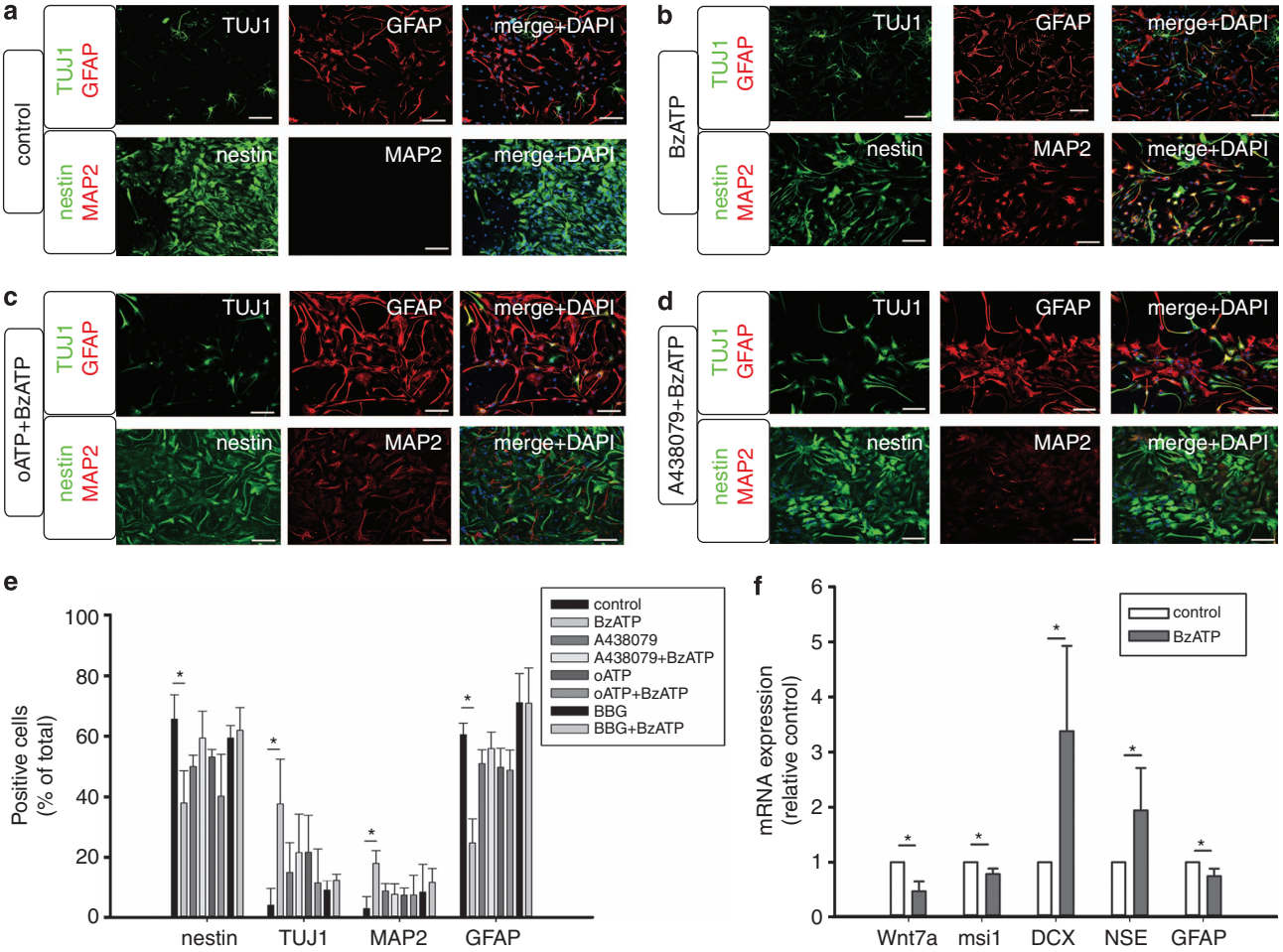

Figure 3 Activation of P2X$_7$R induces the neuronal differentiation of NPCs *in vitro*. Naive (**a**), BzATP-treated (**b**), BzATP + oATP-treated (**c**) and BzATP + A438079-treated (**d**) NPCs were double-stained for TUJ1 (green) and GFAP (red), or nestin (green) and MAP2 (red), and cell nuclei were counterstained with DAPI (blue). Photomicrographs were taken on a confocal microscope ($n = 5$). Scale bar: 10 μM. (**e**) The cells expressing the indicated marker protein and the DAPI-stained cells were counted and were analyzed statistically in the presence of oATP, A438079 or BBG. (**f**) Total RNA of NPCs was isolated, and quantitative RT-PCR analyses were performed to detect mRNA levels of msi1, Wnt7A, GFAP, doublecortin (DCX) or neuronal-specific enolase (NSE) expression in cells treated with or without BzATP. The mRNA transcripts were normalized to the controls ($n = 3$). *$P < 0.05$ using nonpaired Student's *t*-test for comparison with the respective controls

its effects were significantly inhibited by A438079, oATP and BBG (Figure 3e). Furthermore, real-time PCR analysis confirmed that BzATP treatment decreased the mRNA expression of NPCs markers, such as Wnt7a, msi1 and GFAP, but enhanced the expression of neuronal cell markers, such as doublecortin and neuronal-specific enolase (Figure 3f). Thus, activation of $P2X_7Rs$ is likely to enhance neuronal differentiation of NPCs.

To determine whether $P2X_7R$ is involved in the neuronal differentiation of NPCs, we used an shRNA knockdown assay. Full-length $P2X_7R$ was cloned using mRNA isolated from the NPCs and expressed in HEK293T cells. The shRNAs, sR-1133 and sR-135, decreased the $P2X_7R$ mRNA expression in HEK293T-$P2X_7R$ cells (Figure 4a). The shRNAs were infected into NPCs, and we then examined the BzATP-stimulated Ca^{2+} signaling with Ca^{2+} imaging analysis. The statistical analysis of the Ca^{2+} signaling showed that sR1133 and sR-135, but not the scrambled shRNA, significantly blocked the BzATP-induced Ca^{2+} signaling (Figure 4b). We then used immunocytochemical (ICC) to examine the expression of cell markers in these cells. sR-1133 and sR-135, but not sR-Scramble or sR-LacZ, decreased TUJ1 and NeuN expression in the BzATP-treated NPCs and a concomitant increase in nestin and GFAP expression (Figures 4c–f). Thus, we concluded that activation of $P2X_7R$ is involved in neuronal differentiation of NPCs.

The PKC/ERK1/2 pathway regulates NPC differentiation mediated by $P2X_7R$. It is known that the stimulation of $P2X_7R$ induces Ca^{2+} influx[20,21] and the activation of the Ca^{2+}-dependent PKC and ERK1/2.[12,22] In the present study, the time-course analysis revealed that BzATP triggered a rapid ERK1/2 activation that peaked at 3 min and returned to base line levels at 15 min (Figure 5a). The statistical analysis revealed that BzATP triggered a 10-fold increase in p-ERK1/2 (Figure 5b). This effect was blocked by removal of extracellular Ca^{2+} and A438079 (Figures 5c and d). To further examine the components of upstream signaling in ERK1/2 activation, we inhibited MEK, CaMKII, PKC and PI3K, with PD98059, KN93, GF109203X and LY294002, respectively. As shown in Figure 5e, p-ERK1/2 was inhibited by GF109203X and PD98059, but not by KN93 or LY294002. The statistical analysis demonstrated that PD98059 and GF109203X significantly inhibited the BzATP-stimulated ERK1/2 activation (Figure 5f). Together, these results indicated PKC and MEK, but not CaMKII or PI3K, are involved in the $P2X_7R$-mediated ERK1/2 activation, and Ca^{2+}-dependent PKC isozymes may be the upstream signaling to ERK1/2.

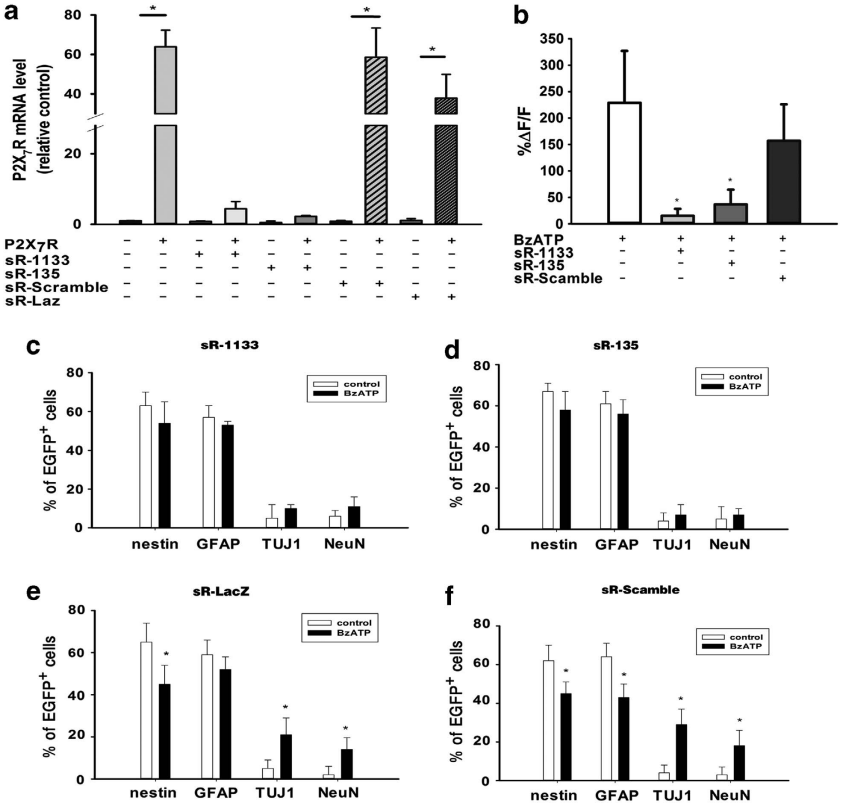

Figure 4 Knockdown of $P2X_7R$ decreases agonist-stimulated neuronal differentiation. (**a**) The lenti-packaged shRNAs, sR-1133, sR-135, sR-Scramble or sR-Laz were infected into HEK293T- or $P2X_7R$-expressing HEK293T (+ $P2X_7R$) cells. Total RNA was isolated and RT-PCR analysis was conducted ($n = 3$); $P2X_7R$ expressed 293T cells. (**b**) Quantitative analyses of BzATP-stimulated $[Ca^{2+}]_i$ in cells infected with sR-1133, sR-135 or sR-Scramble ($n = 3$). *$P < 0.05$ using Mann–Whitney *U*-test for comparison with BzATP. NPCs were infected with sR-1133 (**c**), sR-135 (**d**), sR-LacZ (**e**) or sR-Scramble (**f**), and treated with or without BzATP. The expression of neuronal or NPC markers was examined by ICC ($n = 3$). *$P < 0.05$ using nonpaired Student's *t*-test for comparison with the respective controls

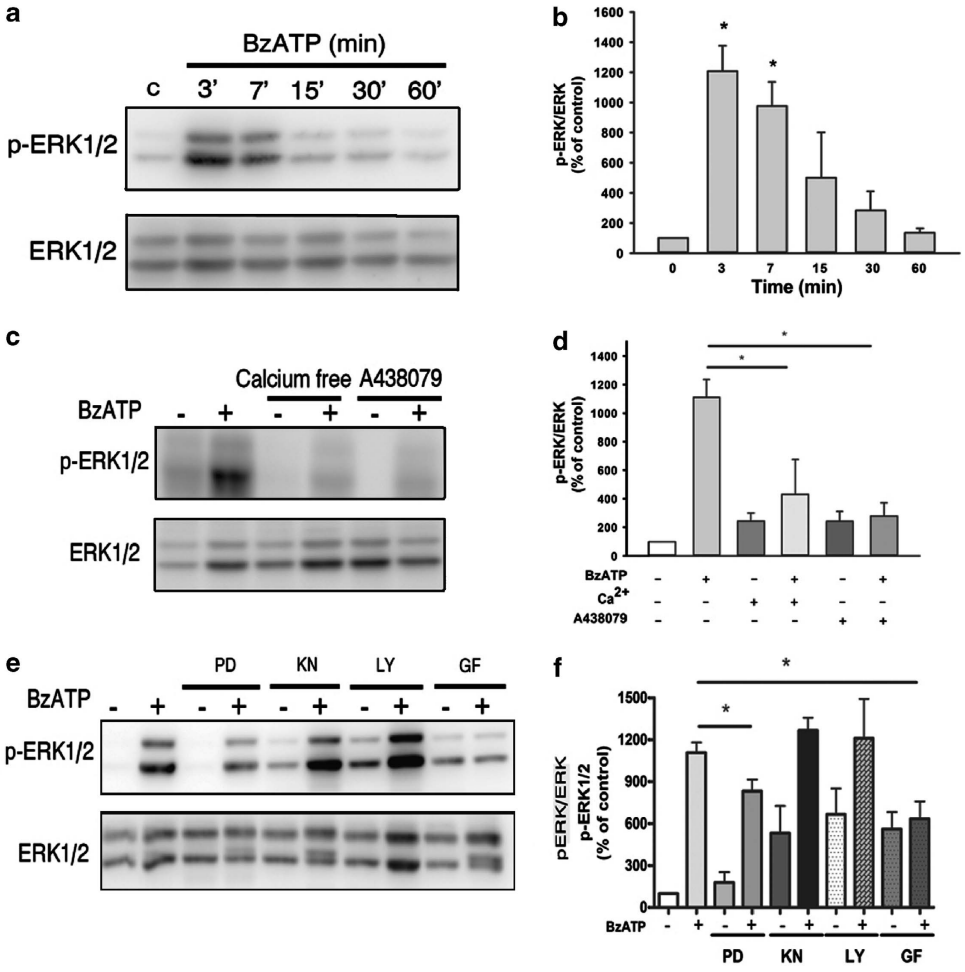

Figure 5 Stimulation of P2X$_7$R activates an ERK1/2 and PKC signaling pathway in NPCs. (**a** and **b**) NPCs were incubated with 50 μM BzATP for 0, 3, 7, 15, 30 and 60 min, and ERK1/2 activation was detected by western blot analysis ($n=3$). *$P<0.05$ using Bonferroni's post test for comparison with the respective controls. Cells were pretreated with 10 μM A438079, 4 mM EGTA (**c**), 10 μM PD98059, 1 μM KN93, 1 μM GF109203X or 10 μM LY294002 (**e**) for 30 min, and were examined for p-ERK1/2 by western blot analysis ($n=3$). *$P<0.05$ using nonpaired Student's *t*-test for comparison with BzATP (**d**–**f**); Calcium free (EGTA), calcium chelator; GF, PKC inhibitor GF109203X; KN, CaMKII inhibitor KN93; LY, PI3K inhibitor LY294002; PD, MEK inhibitor PD98059

We next examined the BzATP-induced translocation of the Ca^{2+}-dependent PKC subtypes. BzATP stimulated increases in the membrane fractions of PKCα and PKCγ but not PKCβ in NPCs (Figure 6a). The statistical analysis revealed that BzATP decreased PKCα and PKCγ but not the PKCβ expression in the cytosolic fraction (Figure 6b), with concomitant increase in membrane fraction (Figure 6c). To ascertain whether PKCα and PKCγ are involved in the ERK1/2 signaling pathway, we used an shRNA knockdown assay. sR-PKCα and sR-PKCγ decreased the expression of PKCα and PKCγ, respectively (Figure 6d). The statistical analysis revealed that sR-PKCα and sR-PKCγ blocked an $\sim$70 and 60% of ERK activation, respectively (Figure 6e). Thus, both PKCα and PKCγ were involved in P2X$_7$R-mediated activation of ERK. To confirm that PKC and ERK1/2 signaling cascade is involved in P2X$_7$R-mediated neuronal differentiation of NPCs, the NPCs were treated with BzATP for 7 days and the number of TUJ1-positive cells was counted. Treatment with either GF109203X or PD98059 partially blocked the BzATP-induced increase in TUJ1-positive cells and increased the number of GFAP-positive cells (Figure 7a). The statistical analysis revealed that effects of PD98059 and GF109203X on BzATP-induced changes in TUJ1 and GFAP expression were significant (Figure 7b). Thus, PKC-ERK1/2 signaling is involved in P2X$_7$R-mediated the neuronal differentiation of NPCs.

Discussion

A previous study showed that P2X$_7$R mRNA is expressed from E14 onward in the rat brain.[6] Similarly, we observed that P2X$_7$R mRNA is expressed in the VZ and SVZ of the E15.5 rat brain. By using the E15.5 brain-derived NPC cultures, we further demonstrated that the potent P2X$_7$R agonist BzATP stimulated Ca^{2+} signaling and induced the neuronal differentiation of these cells. Thus, functional P2X$_7$Rs are expressed in NPC-enriched areas of the embryonic brain.

During development, neuronal differentiation begins at E11.5, peaks at $\sim$E14 and continues at lower levels until E17.5.[23] Our data showed that P2X$_7$R mRNA was expressed

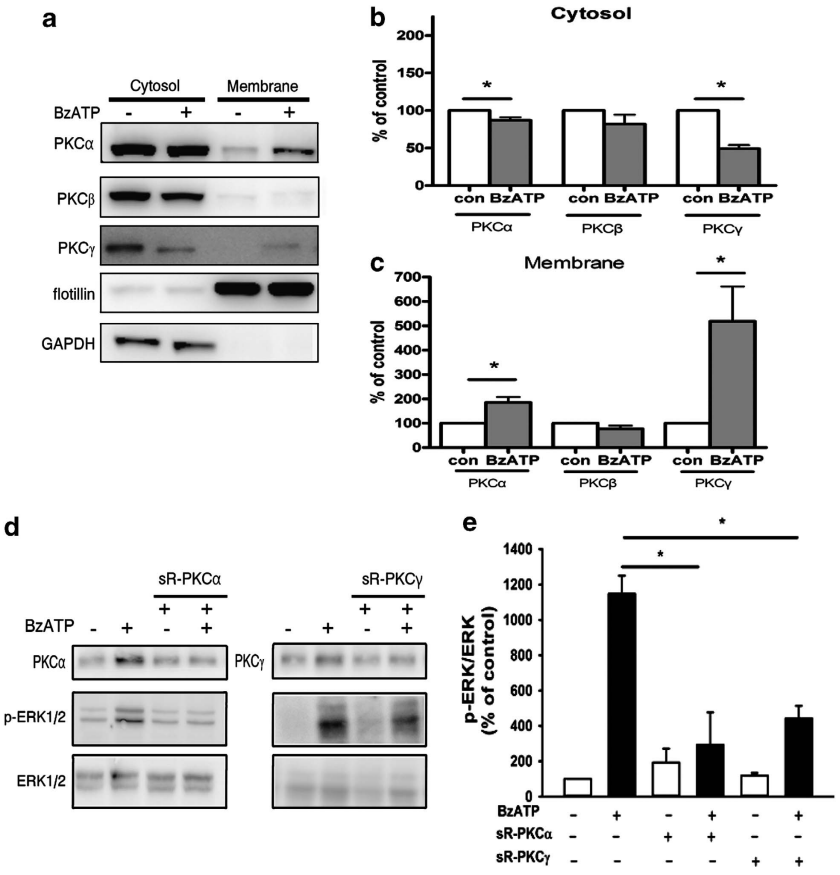

Figure 6 PKCα and PKCγ are associated with P2X$_7$R-mediated ERK1/2 activation in NPCs. (**a**–**c**) NPCs were stimulated with BzATP, and cytosol and membrane fractions were isolated by centrifugation. The expression of Ca^{2+}-dependent conventional PKC isozymes, PKCα, PKCβ and PKCγ, of both membrane and cytosol fractions, was examined by western blot analysis ($n=3$). *$P<0.05$ using nonpaired Student's *t*-test for comparison with the control. (**d**) NPCs were infected with Lenti-packaged shRNAs, sR-PKCα or sR-PKCγ, stimulated with BzATP for 3 min and examined for p-ERK1/2 levels by western blot analysis. (**e**) The ration of p-ERK1/2/ERK1/2 were calculated, using nonpaired Student's *t*-test for comparison with the BzATP ($n=3$)

in the proliferating NPCs of the VZ and SVZ of the E15.5 rat brain. As development proceeded, the P2X$_7$R-expressing differentiating cells moved outwards through the intermediate zone to the cortical plate area. A high level of P2X$_7$R mRNA was observed in the cortical plate area, possibly due to rapid increases in P2X$_7$R-expressing glial cells *in vivo* starting at E17 (Supplementary Figure 1B). However, P2X$_7$R mRNA was also observed in the SVZ and VZ, and throughout the layers of the hippocampus, including the CA1 and CA3 regions, and the SGZ of DG at P4. In adulthood, there is continuous production of new neurons that migrate from the SGZ to the adjacent granule cell layer of the DG.[24] Our results showed the presence of P2X$_7$R mRNA in the DG from E18.5 to adulthood and P2X$_7$R mRNA colocalized with a marker of immature neurons. This suggests that P2X$_7$R expression may be associated with neuronal growth from embryonic stages through adulthood. Recently, P2X$_7$R mRNA was found to be expressed in neurons of the adult rat hippocampus to regulate neurotransmitter release.[25] Our results are consistent with the findings that P2X$_7$Rs are expressed in neurons in the hippocampal area and other regions of the brain.[14,17,26,27]

ATP signaling has been shown to occur during development, both at early stages, such as gastrulation and germ layer definition, and in the late stages of neural development.[28,29] P2X$_7$R expression was initially identified in glial cells in the CNS[20,30,31] and was functionally linked to cytokines and gliotransmitter release.[12,32] Our group showed that P2X$_7$R is involved in proliferation, whereas inhibition and knockdown of the receptor induced neuronal differentiation of N2a neuroblastoma cells.[33] It is known that activation of P2X$_7$R induces a sustained increase in $[Ca^{2+}]_i$ through Ca^{2+} influx. Therefore, P2X$_7$R may act as a mechanism to regulate $[Ca^{2+}]_i$ and control a diverse range of Ca^{2+}-mediated cellular functions. Until now, the roles of cellular ATP signaling and P2X$_7$R in NPCs have remained unexamined. It has been shown that ATP release via hemichannels in retinal pigment epithelium evoked spontaneous elevations of $[Ca^{2+}]_i$ in retinal progenitor cells and in the developing brain.[9,29] Therefore, ATP release may act as an autocrine signal to activate P2X$_7$R and induce Ca^{2+} influx, altering cellular function during development.

It is accepted that ATP is a neurotransmitter in the both central and peripheral nervous systems. ATP is also known to act as a regulator in glia-neuron communication and regulate synaptic transmission and plasticity.[34] ATP is released from nerve terminals via exocytosis and from non-neuronal cells via

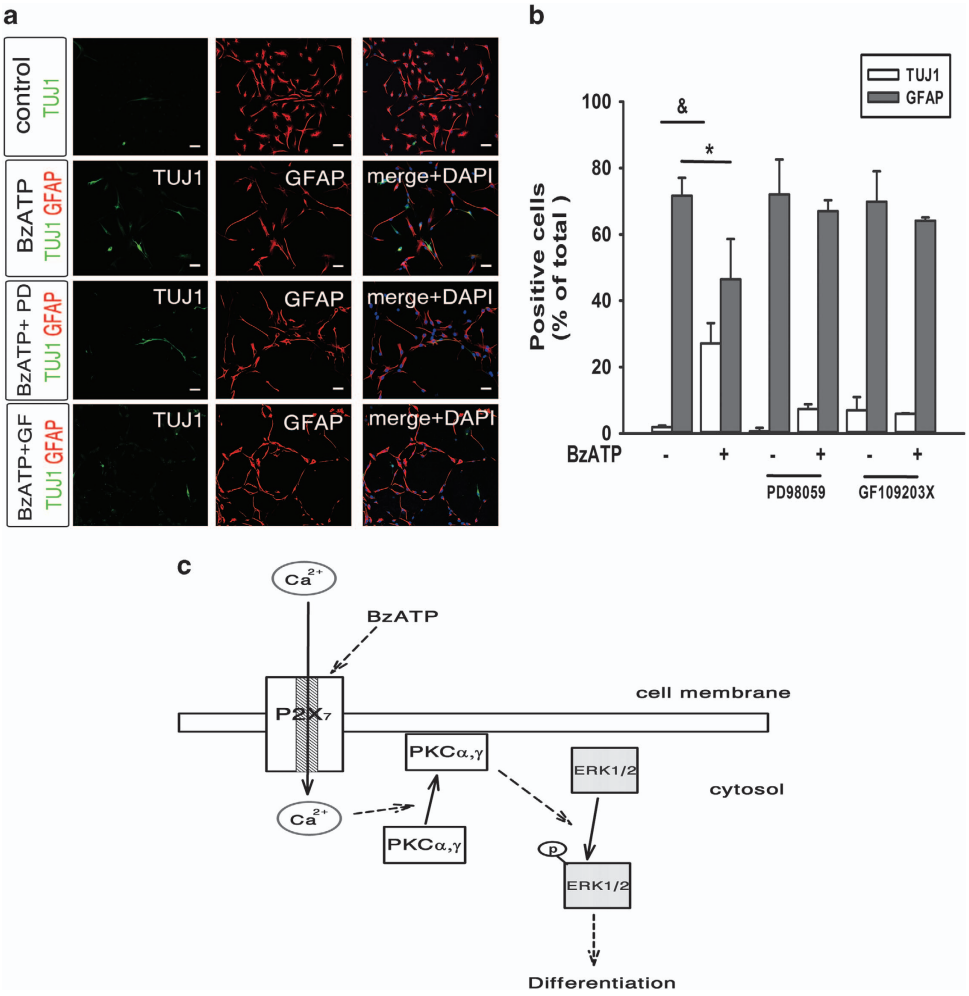

Figure 7 A PKC-ERK signaling pathway is involved in P2X$_7$R-mediated neuronal differentiation of NPCs. (**a**) NPCs were untreated or treated with BzATP, BzATP + PD98059 or BzATP + GF109203X for 7 days, and were then double-stained for GFAP (red) and TUJ1 (green). Cell nuclei were counterstained with DAPI; PD, MEK inhibitor PD98059; GF, PKC inhibitor GF109203X. Scale bar: 10 μM. (**b**) The ratios of fluorescence-positive cells to the DAPI-stained cells per field were measured and are shown as change relative to total cells ($n=3$). $^{\&}P<0.05$, as compared with control for TUJ1 positive cells. $^{*}P<0.05$, as compared with BzATP for GFAP positive cells. (**c**) Schematic drawing of a model for P2X$_7$R activation influence on neuronal differentiation of the NPCs. P2X$_7$R is highly expressed in the membrane of NPCs and its activation triggers Ca^{2+} influx. The uptake of $[Ca^{2+}]_i$ into NPCs activates p-ERK1/2 through the translocation of PKC from the cytosol to membrane, and p-ERK1/2 induces neuronal differentiation

various mechanisms.[35] Presumably, ATP may be released from the NPCs or the neighboring cells to activate P2X$_7$R and other purinergic receptors during development. Our preliminary results showed that NPCs possess several purinergic receptors and that ATP stimulated increases in $[Ca^{2+}]_i$ in these cells (Supplementary Figures 5A and B). Therefore, ATP might activate signaling downstream of Ca^{2+} influx, perhaps through the conventional PKC isozymes in NPCs.

PKC isozymes have been shown to act as upstream regulators of MAPKs.[36,37] Our early results have shown that the stimulation of P2X$_7$R activated PKC and ERK1/2[12,30] and induced the interaction of PKCγ with P2X$_7$R in astrocytes.[38] Similarly, we found that stimulation of P2X$_7$R activated the conventional PKC isozymes PKCα and PKCγ, but not PKCβ, and also activated ERK1/2, but not PI3K and CAMKII, in NPCs. Stimulation of P2X$_7$R was shown to activate a CAMKII-related pathway and to negatively regulate axon[17] and neurite growth.[39] Recently, stimulation of P2X$_7$R induced translocation of PKC-β1 in mouse alveolar epithelial E10 cells.[40] Thus, activation of P2X$_7$R may also activate different intracellular signaling mechanisms to regulate distinct cellular functions in various types of cells.

Prolonged stimulation of P2X$_7$R induces the formation of a non-selective pore and leads to cell death.[41,42] The stimulation of P2X$_7$R in E14.5 NPCs induced cell death in the absence of pore formation.[43] In the present study, the stimulation of P2X$_7$R in E15.5 NPCs triggered neither pore formation nor cell death but did induce neuronal differentiation (Supplementary Figure 5). P2X$_7$R was identified to have survival- and growth-promoting effects in certain cancer cells.[44] In contrast, our earlier result demonstrated that inhibition or knockdown of P2X$_7$R induced neuronal differentiation of N2a neuroblastoma cells.[33] The stimulation of the P2X$_7$R-expressing HEK293 cells increased cell survival in serum-free conditions.[45] Thus, stimulation of P2X$_7$R may lead to alterations of different physiological functions in different types of cells. This

specificity may also be due to different isoforms of P2X$_7$R. Several single-nucleotide polymorphisms with alterations in pathophysiological functions have been identified in human P2X$_7$Rs.[46,47] At least two splice variant isoforms have been identified in mice.[48,49] The P2X$_7$ (k) variant was identified to be constitutively dilated and highly sensitive to agonist BzATP, and escaped gene deletion in one of the P2X$_7$R knockout mouse strains.[48] A recent report also indicated that the ΔC variant is inefficiently trafficked to the cell surface and has little agonist-evoked current.[50] Thus, there are apparent functional and physiological differences between the wild-type receptor and the variants. It is possible that the rat E15.5 NPCs express more than one P2X$_7$R isoform. Further identification of P2X$_7$R isoforms and their physiological functions in NPCs are needed.

NPCs transplantation has been used to deliver therapeutic genes directly to the mouse brain to correct metabolic diseases.[51] The present study not only provides a system to understand the role of P2X$_7$R in brain development but also identifies a signaling pathway with possible therapeutic target sites.

Materials and Methods

Animal tissue preparation. All the experimental animals were approved by the laboratory animal center of the National Yang Ming University (Taipei, Taiwan). The pups were perfused with 0.9% NaCl, followed by fixation with 4% paraformaldehyde (PFA) in phosphate-buffered saline (PBS). The brains were dissected, post-fixed with the same fixative solution for 8 h at 4 °C and then dehydrated in 30% sucrose at 4 °C overnight. All solutions were sterile-filtered and treated with 0.1% diethyl pyrocarbonate. Brain sections were cut into 10-μm slices with a Leica 3050S (Leica Biosystems, Wetzlar, Germany) and were stored at − 80 °C until use. For each experiment, at least three animals were used for each development stage.

Isolation and propagation of embryonic NPCs. Embryonic NPCs were grown according to the method described previously, with modifications.[52] Cells were dissociated from the midbrain and telencephalon without striatum of the E15.5 Sprague–Dawley rat brain and cultured in DMEM/F12 supplemented with N2 (Life Technologies, Frederick, MD, USA),[53] epidermal growth factor (20 ng/ml), basic fibroblast growth factor (10 ng/ml; PeproTech, Rocky Hill, NJ, USA), heparin (5 μg/ml; Sigma-Aldrich, St. Louis, MO, USA) and 50 U/ml penicillin. Neurospheres appeared after 1 week in culture. Medium was replaced every 3 days with gentle trituration, and the spheres were further cultured for 1 month. The cultures were then stained with nestin for the identification of NPCs; 95% of the cells were nestin-positive. After treatment with BzATP (0, 1, 10, 25, 50 and 100 μM) for 4 days, the spheres were mechanically dissociated into single cell, mixed with 0.1% Trypan Blue solution (1:1) and counted immediately with a hemocytometer.

***In vitro* differentiation, cell cycle progress and cell death assay.** To induce differentiation, cells were cultured in DMEM/F12 supplemented with N2 supplement and 0.5% FBS for 2 days.[54,55] Then, fresh differentiation medium with P2X$_7$R agonist, BzATP, was provided for 7 days. To assay for cell cycle progression, neurospheres were dissociated into single-cell suspension and were fixed in 70% (v/v) ethanol at 4 °C for 1.5 h, washed twice with PBS and were stained with propidium iodide (PI) solution (50 μM ribonuclease A, 4 μM PI, 0.1% Triton X-100 in PBS) for 30 min in the dark. Then, cells were assayed with a flow cytometer (FACSCalibur; BD Biosciences, San Diego, CA, USA) and the results were analyzed using FCS Express software (*De Novo* Software, Los Angeles, CA, USA). To assay for cell death, cells were fixed with PFA and analyzed for TUNEL-stained nuclei using a TUNEL kit (Roche, Basel, Switzerland) according to the manufacturer's instructions.

Immunofluorescence staining. For IHC staining, brain sections were treated with 0.1% Triton X-100 in PBS for 20 min, incubated in PBS containing 2% goat serum and 3% horse serum for 1 h, and then incubated with primary antibodies in blocking solution at 4 °C overnight. An ICC analysis was also performed by fixing NPCs in 4% PFA for 20 min, treating with 0.1% Triton X-100 in PBS for 20 min and incubating with primary antibodies at 4 °C overnight before incubation in blocking solution for 1 h. After rinsing three times, the sections or cells were incubated with secondary antibodies conjugated to fluorescein and Texas red (1:200; all from Vector Laboratories) for 2 h and then incubated with 4′-6-diamidino-2-phenylindole (DAPI) for 15 min. Fluorescence signals were detected with a FV300 confocal imaging system (Olympus Japan, Tokyo, Japan). Cell numbers were quantified using NIH ImageJ software. Primary antibodies and dilutions were as follows: GFAP (1:1000; DAKO, Glostrup, Denmark), Nestin (1:200; Millipore, Bedford, MA, USA), NeuN (1:200; Chemicom, Temecula, CA, USA), MAP2 (1:300; Chemicom) and β-tubulin type III monoclonal (TUJ1, 1:1000; Promega, Southampton, UK).

***In vitro* transcription.** The P2X$_7$R probe was cloned into pGEM T-easy vector (Promega) for the antisense and sense riboprobe synthesis. The non-radioactive riboprobes were synthesized by *in vitro* transcription using T7 and SP6 polymerase (Promega), respectively, and were labeled with digoxigenin-labeling mix (Roche). Before hybridization, the riboprobes were diluted with the hybridization buffer to 2 ng/μl and denatured at 65 °C for 10 min. A 119 bp cDNA fragment of the P2X$_7$R corresponds to bases from 1258 to 1376 (numbering a according to GenBank accession number no. X95882).

ISH of P2X$_7$R mRNA expression. Brain sections were fixed with 4% PFA, treated with 0.2 N HCl and l μg/ml protease K, and then incubated with prehybridization buffer containing 50% formamide and 2 × SSC at 60 °C for 90 min. The sections were hybridized with digoxigenin-labeled riboprobes in hybridization buffer (10% dextran sulfate, 50% formamide, 1 mM EDTA, 318 mM NaCl, 10.6 mM Tris, 1 × Denhardt's solution, 500 μg/ml tRNA and 10 mM DTT) at 60 °C for 16 h, washed with 50% formamide in 2 × SSC at 60 °C for 1 h, 20 μg/ml RNaseA for 30 min, and then washed sequentially with 2 × SSC and 0.2 × SSC at 60 °C for 20 min. The sections were blocked with 2% blocking reagent containing 8% sheep serum in TNT buffer (100 mM Tris, pH 7.5, 150 mM NaCl and 0.05% Tween-20) for 1 h. The endogenous peroxidases were inhibited with 0.3% H_2O_2 in PBS for 10 min and the sections were then incubated with POD-conjugated sheep anti-digoxigenin antibody (1:1000, Roche) for 3 h. After washing with TNT buffer twice, the signals were detected by using TSA PLUS Fluorescence Kits (1:700, PerkinElmer, Norwalk, CT, USA).

Protein fractionation, immunohistology analysis and western blot. For western blot analysis, proteins were extracted by scraping the NPCs in homogenate buffer (320 mM sucrose, 1 mM EDTA, 50 mM Tris-HCl, 1 mM PMSF and 1 × proteinase inhibitor). After homogenation on ice, cell lysates were cleared by centrifugation at 1000 × *g* in a microcentrifuge (Kubota, Tokyo, Japan) for 10 min at 4 °C. The supernatant were then centrifuged at 100 000 × *g* in a desktop ultracentrifuger (Beckman Coulter, Fullerton, CA, USA). The cytosolic fraction was taken from the supernatants after centrifugation and the membrane fraction from the pellets was lysed in lysis buffer (20 mM HEPES, 1% Triton X-100, 10 mM NaF, 1 mM Na_3VO_4, 1 mM PMSF). Aliquots of proteins (20 μg) proteins were separated by 10% SDS-PAGE, transferred onto PVDF membrane and incubated overnight with 5% BSA in PBS. The membranes were incubated with primary antibodies, followed by hybridized with the HRP-conjugated secondary antibody (1:10000; Vector Laboratories). The membranes were reacted with Luminata Western HRP Substrates (Millipore) and detected with a digital image system (ImageQuant LAS 4000; Fujifilm Lifescience, Tokyo, Japan). The primary antibodies contained phospho-p44/42 MAPK (p-ERK1/2; 1:400), p44/42 MAPK (ERK1/2; 1:200) and glyceraldehyde-3-phosphate dehydrogenase (GAPDH; 1:1000), purchased from Cell Signaling Technology (Danvers, MA, USA). PKCα (1:500), PKCβ (1:250), PKCγ (1:500) and flotillin (1:1000) antibodies were purchased from BD Biosciences.

Reverse-transcription PCR. Total RNA was extracted from NPCs with 1 ml of Rezol reagent (Protech Technologies, Taipei, Taiwan). One milligram of total RNA was reverse-transcribed using Superscript III reverse transcriptase (Life Technologies) in 20 μl at 42 °C for 1 h according to the manufacturer's protocol. Primer 3 software (http://frodo.wi.mit.edu) was used to design oligonucleotide primers spanning intron sequences, and these primers are listed in Table 1.

Table 1 Cell markers and purinergic receptor primers used for RT-PCR and Q-PCR analysis

Gene	Forward primer (5′–3′)	Reverse primer (5′–3′)	Product length (bp)
Gfap	GACTTTCTCCAACCTCCAG	TCTCCACCGTCTTTACCA	98
Dcx	GCAGTCAGCTCTCAACAC	GACAGTGGCAGGTACAAG	100
Gapdh	ACTCCCATTCTTCCACCT	CATGTAGGCCATGAGGTC	128
Msi1	GGTTACACCTACCAGTTCCC	GCCATCGGACCATAAGCA	110
Wnt7a	CTTCGCCAAGGTCTTCGT	ACTCCAGTTTCATGTTCTCCTC	116
NSE	GAACTATCCTGTGGTCTCC	CGACATTGGCTGTGAACTTG	80
P2rx7 full	ATACGGACCGATGCCGGCTTGC	CGGACCGTCAGTAGGGATACTTGAAG	1805
P2rx1	GGGATTGGCATCTTTGGAG	CCCATGTCCTCGGCATATT	113
P2rx2	CAGTCTCATTCCCACCATC	GTCACAGGCCATCTACTTGA	174
P2rx3	GCACTGTTCTCTGTGACATC	CTGTAGACTGCTTCTCCACA	162
P2rx4	GCTGGGAAGTTTGACATC	TGCAGTAGAGGACTATGACG	103
P2rx5	CCAATGTTGAGGTTGAGG	CTACGTCTTCACTGGATGC	221
P2rx6	GTCACCTTCCTCTGTGATCT	GTTGGTAGTTGCCTTTGG	105
P2rx7	AGTCTGCAAGATGTCAAAGG	ATTTCCTCAGGTTGTCCAG	119
P2ry1	ATCTCCCCCATTCTCTTCTA	TAAACCCTGTCGTTGAAATC	362
P2ry2	GGCAGTTTCTGACTCTCTCT	CACTAGCACCCACACAAC	259
P2ry4	ACCCGCACAATTTATTACC	TGCTGATGCTTTCCTCAT	250
P2ry6	TTATCAGCTTCCTGCCTTT	GCTTCTGTAGGAGATCGTGT	210

Quantitative real-time PCR. Real-time PCR analyses were performed on the Rotor-Gene 3000 (Qiagen, Valencia, CA, USA) using the SYBR Fast One-Step qRT-PCR Kit (Kapa Biosystems, Woburn, MA, USA) and the manufacturer's protocol. Specific primers were designed by Primers 3 software and are listed in Table 1. The melting curve detected a single melt peak and PCR efficiency values between 90 and 110% for all amplicons. Relative gene expression levels were then normalized to GAPDH expression in each sample.

BrdU incorporation assay. The BrdU incorporation assay was performed by using the Cell Proliferation BrdU kit (Roche). After the experiment, the cells were labeled with a 10 mM BrdU solution and incubated for 8 h at 37 °C, washed with PBS, fixed with FixDenat for 30 min and incubated in 1 N HCl for 10 min at 4 °C. The cells were then washed with PBS with 1% Triton X-100, neutralized with 0.1 M $Na_2B_4O_7$ for 12 min and then blocked with 2% goat serum for 1 h. After rinsing with PBS, the cells were incubated with anti-BrdU-POD antibody (1:300) for 2 h, and the signals were detected with TSA PLUS Fluorescence kits.

Construction of expression plasmids. The pGEM-P2X$_7$ plasmid was constructed by inserting the full fragment of the rat P2X$_7$R sequence (number X95882) into the pGEM-T Easy vector (Promega). The primer is listed in Table 1. The fragments were generated by HiFi DNA polymerase (Yeastern Biotech, Shijr, Taiwan). The conditions were as follows: denaturation at 94 °C for 1 min followed by 30 cycles of denaturation at 94 °C for 15 s, annealing at 60 °C for 30 s and extension at 68 °C for 2 min followed by at 68 °C for 5 min. The products were cloned into a pGEM T-easy vector, and then the plasmid DNA was transfected into HEK293T cells with the Lipofectamine 2000 transfection method according to the manufacturer's procedure (Life Technologies). HEK293T cells were grown in DMEM (Life Technologies) medium with 10% FBS.

shRNA knockdown. shRNA targeting P2X$_7$R mRNA was purchased from Biosettia (San Diego, CA, USA). The sequences are as follows: non-specific shRNA (sR-LacZ) 5′-GCAGTTATCTGGAAGATCAGG-CCTGATCTTCCAGA TAACTGC-3′, sh-P2X$_7$–135 (sR-135) 5′-GCAGCTGGAACGATGTCTTTC-GAAA GACATCGTTCCAGCTGC-3′, sh-P2X$_7$–1133 (sR-1133) 5′-GGATCCACCCTG TCCTATTTC-GAAATAGGACAGGGTGGATCC-3′ and sh-P2X$_7$-scramble shRNA (sR-Scramble) 5′-GCTACACTATCGAGCAATT-AATTGCTCGATAGTGTAGC-3′. All shRNA sequences have 5′-TTGGATCCAA-3′ in the sequence for the short-hairpin loop. The pLV-RNAi vector contains a mouse U6 promoter-driven shRNA coding sequence followed by a CMV-driven EGFP reporter. HEK293T cells expressing pGEM-P2X$_7$ plasmid or NPCs were infected with sR-Scramble, sR-1133, sR-LacZ or sR-135, and the desired virus titer was reached when cells were infected at an MOI of 0.5. PKCα and PKCγ shRNA clones were obtained from the National RNAi Core Facility (Genomics Research Center, Academia Sinica, Taiwan). shRNA against the target sequence was sR-PKCα for mouse PKCα (clone ID TRCN0000235973) and sR-PKCγ for human PKCγ (TRCN0000199230).

Ca^{2+} image analysis. Cells were grown on 24-mm coverslips and were incubated with loading buffer (125 mM NaCl, 5 mM KCl, 1.8 mM $CaCl_2$, 2 mM $MgCl_2$, 0.5 mM NaH_2PO_4, 5 mM $NaHCO_3$, 10 mM HEPES and 10 mM glucose, pH 7.4) containing 1 μg/ml Fura-2 AM (Life Technologies) for 40 min at 37 °C in the dark. Ca^{2+} imaging analysis was performed using excitation wavelengths (340/380 nm) selected by means of a computer-controlled rotating filter wheel between a xenon light source and the microscope. The resulting image at each wavelength was averaged in real time, digitalized and stored in an image-processing unit. The results were calculated using a Metafluor image analysis system (Universal Imaging Corporation, Philadelphia, PA, USA). Statistical analysis was conducted after the calculation of changes in fluorescence (ΔF) and expressed as percentage of the average baseline fluorescence (F) (%ΔF/F).[56]

Statistical analysis. All statistical analyses were performed using SAS Version 9.1.3 (SAS Institute, Cary, NC, USA) and SigmaPlot XII Software (Systat Software, San Jose, CA, USA). Results are represented as the mean $\pm$ S.D. and the symbol * indicates significantly different means ($P<0.05$) as analyzed by a nonpaired Student's *t*-test or one-way ANOVA with Bonferroni's *post-hoc* test. The Mann–Whitney's *U*-test with nonparametric distribution was used to compare peak values of Ca^{2+}.

Conflict of Interest

The authors declare no conflict of interest.

Acknowledgements. This work was supported by grants NSC 100-2321-B-010-005 from the National Science Council of Taiwan, ROC, and 101AC-B5 and 102AC-B5 from the Ministry of Education of Taiwan Aim for the Top University Plan.

1. Edlund T, Jessell TM. Progression from extrinsic to intrinsic signaling in cell fate specification: a view from the nervous system. *Cell* 1999; **96**: 211–224.
2. Rietze RL, Valcanis H, Brooker GF, Thomas T, Voss AK, Bartlett PF. Purification of a pluripotent neural stem cell from the adult mouse brain. *Nature* 2001; **412**: 736–739.
3. Pencea V, Luskin MB. Prenatal development of the rodent rostral migratory stream. *J Comparative Neurol* 2003; **463**: 402–418.
4. Götz M, Huttner WB. The cell biology of neurogenesis. *Nat Rev Mol Cell Biol* 2005; **6**: 777–788.
5. Kempermann G, Jessberger S, Steiner B, Kronenberg G. Milestones of neuronal development in the adult hippocampus. *Trends Neurosci* 2004; **27**: 447–452.
6. Cheung KK, Chan WY, Burnstock G. Expression of P2X purinoceptors during rat brain development and their inhibitory role on motor axon outgrowth in neural tube explant cultures. *Neuroscience* 2005; **133**: 937–945.
7. Lin JH, Takano T, Arcuino G, Wang X, Hu F, Darzynkiewicz Z *et al.* Purinergic signaling regulates neural progenitor cell expansion and neurogenesis. *Dev Biol* 2007; **302**: 356–366.

8. Salter MW, Hicks JL. ATP causes release of intracellular Ca2 + via the phospholipase C beta/IP3 pathway in astrocytes from the dorsal spinal cord. *J Neurosci* 1995; **15**: 2961–2971.
9. Pearson RA, Dale N, Llaudet E, Mobbs P. ATP released via gap junction hemichannels from the pigment epithelium regulates neural retinal progenitor proliferation. *Neuron* 2005; **46**: 731–744.
10. Hassenklöver T, Schwartz P, Schild D, Manzini I. Purinergic signaling regulates cell proliferation of olfactory epithelium progenitors. *Stem Cells* 2009; **27**: 2022–2031.
11. Surprenant A, Rassendren F, Kawashima E, North RA, Buell G. The cytolytic P2Z receptor for extracellular ATP identified as a P2X receptor ($P2X_7$). *Science* 1996; **272**: 735–738.
12. Wang CM, Chang YY, Sun SH. Activation of $P2X_7$ purinoceptor-stimulated TGF-beta 1 mRNA expression involves PKC/MAPK signalling pathway in a rat brain-derived type-2 astrocyte cell line, RBA-2. *Cell Signal* 2003; **15**: 1129–1137.
13. Iglesias R, Locovei S, Roque A, Alberto AP, Dahl G, Spray DC *et al.* $P2X_7$ receptor-Pannexin1 complex: pharmacology and signaling. *Am J Physiol Cell Physiol* 2008; **295**: C752–C760.
14. Deuchars SA, Atkinson L, Brooke RE, Musa H, Milligan CJ, Batten TF *et al.* Neuronal $P2X_7$ receptors are targeted to presynaptic terminals in the central and peripheral nervous systems. *J Neurosci* 2001; **21**: 7143–7152.
15. Miras-Portugal MT, Díaz-Hernández M, Giráldez L, Hervás C, Gómez-Villafuertes R, Sen RP *et al.* $P2X_7$ receptors in rat brain: presence in synaptic terminals and granule cells. *Neurochem Res* 2003; **28**: 1597–1605.
16. Peng W, Cotrina ML, Han X, Yu H, Bekar L, Blum L *et al.* Systemic administration of an antagonist of the ATP-sensitive receptor $P2X_7$ improves recovery after spinal cord injury. *Proc Natl Acad Sci USA* 2009; **106**: 12489–12493.
17. Díaz-Hernandez M, del Puerto A, Díaz-Hernandez JI, Diez-Zaera M, Lucas JJ, Garrido JJ *et al.* Inhibition of the ATP-gated $P2X_7$ receptor promotes axonal growth and branching in cultured hippocampal neurons. *J Cell Sci* 2008; **121**: 3717–3728.
18. Weissman TA, Riquelme PA, Ivic L, Flint AC, Kriegstein AR. Calcium waves propagate through radial glial cells and modulate proliferation in the developing neocortex. *Neuron* 2004; **43**: 647–661.
19. Hogg RC, Chipperfield H, Whyte KA, Stafford MR, Hansen MA, Cool SM *et al.* Functional maturation of isolated neural progenitor cells from the adult rat hippocampus. *Eur J Neurosci* 2004; **19**: 2410–2420.
20. Suadicani SO, Brosnan CF, Scemes E. $P2X_7$ receptors mediate ATP release and amplification of astrocytic intercellular Ca^{2+} signaling. *J Neurosci* 2006; **26**: 1378–1385.
21. Donnelly-Roberts DL, Namovic MT, Han P, Jarvis MF. Mammalian $P2X_7$ receptor pharmacology: comparison of recombinant mouse, rat and human $P2X_7$ receptors. *Br J Pharmacol* 2009; **157**: 1203–1214.
22. Hung AC, Sun SH. The $P2X_7$ receptor-mediated phospholipase D activation is regulated by both PKC-dependent and PKC-independent pathways in a rat brain-derived Type-2 astrocyte cell line, RBA-2. *Cell Signal* 2002; **14**: 83–92.
23. Ghosh A, Greenberg ME. Distinct roles for bFGF and NT-3 in the regulation of cortical neurogenesis. *Neuron* 1995; **15**: 89–103.
24. Zhao C, Deng W, Gage FH. Mechanisms and functional implications of adult neurogenesis. *Cell* 2008; **132**: 645–660.
25. Sperlágh B, Köfalvi A, Deuchars J, Atkinson L, Milligan CJ, Buckley NJ *et al.* Involvement of $P2X_7$ receptors in the regulation of neurotransmitter release in the rat hippocampus. *J Neurochem* 2002; **81**: 1196–1211.
26. Cho JH, Choi IS, Jang IS. $P2X_7$ receptors enhance glutamate release in hippocampal hilar neurons. *Neuroreport* 2010; **21**: 865–870.
27. del Puerto A, Díaz-Hernández JI, Tapia M, Gomez-Villafuertes R, Benitez MJ, Zhang J *et al.* Adenylate cyclase 5 coordinates the action of ADP, $P2Y_1$, $P2Y_{13}$ and ATP-gated $P2X_7$ receptors on axonal elongation. *J Cell Sci* 2012; **125**: 176–188.
28. Burnstock G, Ulrich H. Purinergic signaling in embryonic and stem cell development. *Cell Mol Life Sci* 2011; **68**: 1369–1394.
29. Dale N. Dynamic ATP signalling and neural development. *J Physiol* 2008; **586**: 2429–2436.
30. Sun SH, Lin LB, Hung AC, Kuo JS. ATP-stimulated Ca^{2+} influx and phospholipase D activities of a rat brain-derived type-2 astrocyte cell line, RBA-2, are mediated through $P2X_7$ receptors. *J Neurochem* 1999; **73**: 334–343.
31. Rappold PM, Lynd-Balta E, Joseph SA. $P2X_7$ receptor immunoreactive profile confined to resting and activated microglia in the epileptic brain. *Brain Res* 2006; **1089**: 171–178.
32. Sun SH. Roles of $P2X_7$ receptor in glial and neuroblastoma cells: the therapeutic potential of $P2X_7$ receptor antagonists. *Mol Neurobiol* 2010; **41**: 351–355.
33. Wu PY, Lin YC, Chang CL, Lu HT, Chin CH, Hsu TT *et al.* Functional decreases in $P2X_7$ receptors are associated with retinoic acid-induced neuronal differentiation of Neuro-2a neuroblastoma cells. *Cell Signal* 2009; **21**: 881–891.
34. Fields RD, Burnstock G. Purinergic signalling in neuron-glia interactions. *Nat Rev Neurosci* 2006; **7**: 423–436.
35. Bodin P, Burnstock G. Purinergic signalling: ATP release. *Neurochem Res* 2001; **26**: 959–969.
36. Belcheva MM, Clark AL, Haas PD, Serna JS, Hahn JW, Kiss A *et al.* Mu and kappa opioid receptors activate ERK/MAPK via different protein kinase C isoforms and secondary messengers in astrocytes. *J Biol Chem* 2005; **280**: 27662–27669.
37. Geraldes P, Hiraoka-Yamamoto J, Matsumoto M, Clermont A, Leitges M, Marette A *et al.* Activation of PKC-delta and SHP-1 by hyperglycemia causes vascular cell apoptosis and diabetic retinopathy. *Nat Med* 2009; **15**: 1298–1306.
38. Hung AC, Chu YJ, Lin YH, Weng JY, Chen HB, Au YC *et al.* Roles of protein kinase C in regulation of $P2X_7$ receptor-mediated calcium signalling of cultured type-2 astrocyte cell line, RBA-2. *Cell Signal* 2005; **17**: 1384–1396.
39. Gómez-Villafuertes R, del Puerto A, Díaz-Hernández M, Bustillo D, Díaz-Hernández JI, Huerta PG *et al.* Ca^{2+}/calmodulin-dependent kinase II signalling cascade mediates $P2X_7$ receptor-dependent inhibition of neuritogenesis in neuroblastoma cells. *FEBS J* 2009; **276**: 5307–5325.
40. Bläsche R, Ebeling G, Perike S, Weinhold K, Kasper M, Barth K. Activation of $P2X_7R$ and downstream effects in bleomycin treated lung epithelial cells. *Int J Biochem Cell Biol* 2012; **44**: 514–524.
41. Virginio C, MacKenzie A, Rassendren FA, North RA, Surprenant A. Pore dilation of neuronal P2X receptor channels. *Nat Neurosci* 1999; **2**: 315–321.
42. North RA. Molecular physiology of P2X receptors. *Physiol Rev* 2002; **82**: 1013–1067.
43. Delarasse C, Gonnord P, Galante M, Auger R, Daniel H, Motta I *et al.* Neural progenitor cell death is induced by extracellular ATP via ligation of $P2X_7$ receptor. *J Neurochem* 2009; **109**: 846–857.
44. Thompson BA, Storm MP, Hewinson J, Hogg S, Welham MJ, MacKenzie AB. A novel role for $P2X_7$ receptor signalling in the survival of mouse embryonic stem cells. *Cell Signal* 2012; **24**: 770–778.
45. Adinolfi E, Callegari MG, Ferrari D, Bolognesi C, Minelli M, Wieckowski MR *et al.* Basal activation of the $P2X_7$ ATP receptor elevates mitochondrial calcium and potential, increases cellular ATP levels, and promotes serum-independent growth. *Mol Biol Cell* 2005; **16**: 3260–3272.
46. Wiley JS, Dao-Ung LP, Li C, Shemon AN, Gu BJ, Smart ML *et al.* An Ile-568 to Asn polymorphism prevents normal trafficking and function of the human $P2X_7$ receptor. *J Biol Chem* 2003; **278**: 17108–17113.
47. Cabrini G, Falzoni S, Forchap SL, Pellegatti P, Balboni A, Agostini P *et al.* A His-155 to Tyr polymorphism confers gain-of-function to the human $P2X_7$ receptor of human leukemic lymphocytes. *J Immunol* 2005; **175**: 82–89.
48. Nicke A, Kuan YH, Masin M, Rettinger J, Marquez-Klaka B, Bender O *et al.* A functional $P2X_7$ splice variant with an alternative transmembrane domain 1 escapes gene inactivation in $P2X_7$ knock-out mice. *J Biol Chem* 2009; **284**: 25813–25822.
49. Ohlendorff SD, Tofteng CL, Jensen JE, Petersen S, Civitelli R, Fenger M *et al.* Single nucleotide polymorphisms in the $P2X_7$ gene are associated to fracture risk and to effect of strogen treatment. *Pharmacogenet Genomics* 2007; **17**: 555–567.
50. Masin M, Young C, Lim K, Barnes SJ, Xu XJ, Marschall V *et al.* Expression, assembly and function of novel C-terminal truncated variants of the mouse $P2X_7$ receptor: re-evaluation of $P2X_7$ knockouts. *Br J Pharmacol* 2012; **165**: 978–993.
51. Snyder EY, Taylor RM, Wolfe JH. Neural progenitor cell engraftment corrects lysosomal storage throughout the MPS VII mouse brain. *Nature* 1995; **374**: 367–370.
52. Zhou FC, Kelley MR, Chiang YH, Young P. Three to four-year-old nonpassaged EGF-responsive neural progenitor cells: proliferation, apoptosis, and DNA repair. *Exper Neurol* 2000; **164**: 200–208.
53. Bottenstein JE, Sato GH. Growth of a rat neuroblastoma cell line in serum-free supplemented medium. *Proc Natl Acad Sci USA* 1979; **76**: 514–517.
54. Takahashi M, Palmer TD, Takahashi J, Gage FH. Widespread integration and survival of adult-derived neural progenitor cells in the developing optic retina. *Mol Cell Neurosci* 1998; **12**: 340–348.
55. Song H, Stevens CF, Gage FH. Astroglia induce neurogenesis from adult neural stem cells. *Nature* 2002; **417**: 39–44.
56. Grynkiewicz G, Poenie M, Tsien RY. A new generation of Ca2 + indicators with greatly improved fluorescence properties. *J Biol Chem* 1985; **260**: 3440–3450.

Supplementary Information accompanies this paper on Cell Death and Disease website (http://www.nature.com/cddis)